Enhancing Drug-Drug Interaction Prediction by Integrating Physiologically-Based Pharmacokinetic Model with Fraction Metabolized by CYP3A4

Pin Jiang[1], Tao Chen[2], Lin-Feng Chu[1], Ren-peng Xu[1], Jin-Ting Gao[3], Li Wang[3], Qiang Liu[3], Lily Tang[3], Hong Wan[1], Ming Li[4], and Ren Hong-can[3]

[1]Shanghai Medicilon Inc
[2]Shanghai PharmoGo Co., Ltd.
[3]GenFleet Therapeutics (Shanghai) Inc
[4]The First Affiliated Hospital of Zhengzhou University

April 17, 2023

Abstract

ABSTRACT BACKGROUND AND PURPOSE Enhancing the precision of drug-drug interaction (DDI) prediction is essential for mitigating potential drug interactions and enhancing drug safety and efficacy. This study aims to investigate the impact of in vitro and in silico approaches for calculating the fraction metabolized by CY3A4 (fm) on DDI prediction accuracy and identified the most effective method for improving DDI prediction using physiologically based pharmacokinetic (PBPK) models. EXPERIMENTAL APPROACH Both in vitro and in silico methods were utilized to determine fm values for 33 approved drugs, or fm values were assumed to be 100%. These fm values were then integrated into PBPK models. Subsequently, the PBPK models were combined with a PBPK model of ketoconazole to predict potential DDIs. Finally, the accuracy of these predictions was assessed. KEY RESULTS The integration of in vitro fm had remarkable precision in predicting CmaxR of 31 drugs and accurately predicting AUCRs of 28 drugs out of 33 drugs, both within 2 times of the measured values. However, using 100% fm and in silico fm resulted in lower prediction accuracy that was comparable to each other. CONCLUSIONS AND IMPLICATIONS Our study highlights the importance of incorporating in vitro fm data into PBPK models to improve the accuracy of predicting DDIs. While in silico fm may have some potential, its influence on predictions appears to be limited. Additionally, our findings suggest that drugs with high Clliver levels (>15 L·h-1) and high fm (>75%) are particularly susceptible to the impact of CYP3A4 inhibitor ketoconazole.

INTRODUCTION

Combined drug therapies have become increasingly popular in recent years due to their ability to simultaneously treat multiple conditions with a personalized combination of drugs (Gertz & Dispenzieri, 2020; Lu et al., 2017). However, the potential for drug-drug interactions (DDIs) to cause adverse effects and serious safety issues is a concern. In particular, when a perpetrator drug inhibits the metabolism of victim drugs via the CYP3A enzyme, it can lead to an increase in exposure of the victim drugs. To minimize the risk of negative effects from DDIs, the potential for interaction between perpetrator and victim drugs can be assessed during the drug discovery and development process and after the drug has been approved (Yang, Pfuma Fletcher, Huang, Zineh & Madabushi, 2021). A mechanistic static model can be used to evaluate the ratio of the concentration-time area under the curve (AUC) for a test article (i.e. a drug) after co-administration with a perpetrator of CYP3A to the AUC for the test article after dosing alone (AUCR, AUCi/AUC) (Gomez-Mantilla, Huang & Peters, 2023). If this ratio is found to be greater than the traditional threshold of 1.25, it is considered an indicator of a potential DDI, and further studies are performed to evaluate the DDI risk.

However, static models have limitations in that they use a single concentration of a drug and can over-predict the extent of DDI. Dynamic models that take into account the time-varying concentrations of drugs and metabolites may provide a more accurate assessment of DDIs.

Physiologically based pharmacokinetic (PBPK) modeling is widely adopted by the pharmaceutical industry for evaluating DDIs due to its ability to consider the time-course of drug concentrations, resulting in more accurate predictions (Lin, Chen, Unadkat, Zhang, Wu & Heimbach, 2022). If the PBPK model can predict the observed DDI accurately, and sensitivity analysis indicates minimal impact, a clinical DDI study may not be necessary (Shebley et al., 2018). However, the decision to conduct such a study ultimately depends on various factors, such as regulatory requirements, the potential consequences of the DDI, the stage of drug development, and the predictive performance (accuracy and reliability) of the PBPK-DDI model. To evaluate the predictive performance of the PBPK model for DDIs, we used the PBPK model to predict the DDIs of 35 substrates after co-administration with an inhibitor, and then compare them with the observed results (Ren, Sai, Chen, Zhang, Tang & Yang, 2021). The comparison revealed that 75% of the predicted AUCR values by the model were within a 2-fold range of the observed AUCR values, with the assumption of 100% of the fraction metabolized (f_m). This preliminary analysis suggests that incorporating reported "f_m " into the prediction model for certain drugs (crizotinib, macitentan, panobinostate, and ruxolitinib) could result in improved accuracy. However, further testing on f_m and an expanded study with a larger sample size are necessary to accurately evaluate the improvement in predictive performance.

A commonly used method for quantifying $f_m$involves conducting an *in vitro* assay using human liver microsomes (HLM). This assay requires incubating a compound with HLM in the presence and absence of an inhibitor of interest and determining the clearance (Cl_{int}) of the compound under both conditions (Murayama et al., 2018). HLM are a prevalent *in vitro* model for determining drug metabolism or f_m , as they are affordable and cost-effective. In addition to traditional methods such as *in vitro* or *in vivo* testing, in silico methods can be employed to predict the fate of molecules in the body through computer simulations (Watanabe et al., 2023). These methods are generally more economical. In this paper, we will describe the use of both *in vitro* and in silico methods to determine $f_m$values. We will then use these values to update previous PBPK models of the substrates and further predict DDIs. Finally, we will evaluate the accuracy of the different methods used.

Materials and methods

The methods section is divided into two parts. The first part outlines the technical details of *in vitro* platform testing fraction metabolized. The second part provides a detailed description of the data analysis, including (i) the development and validation of the PBPK-DDI model, (ii) the prediction of the DDIs of 33 compounds, and (iii) an evaluation of the predictive performance.

Part I

Chemical and reagents

The following compounds were obtained from Aladdin: Fostamatinib (Lot No.: J1508085), Ponatinib (Lot No.: F1511088), Axitinib (Lot No.: I1410008), Crizotinib (Lot No.: I1828093), Venetoclax (Lot No.: C1608065), Ibrutinib (Lot No.: C1808046), Nintedanib (Lot No.: G1524093), Rivaroxaban (Lot No.: E1522122), Apixaban (Lot No.: D2007114), Ospemifene (Lot No.: F1702014), Roflumilast (Lot No.: I1828049), Suvorexant (Lot No.: H1504094), Vilazodone (Lot No.: E1712149), Apremilast (Lot No.: B2102013), Elagolix (Lot No.: K2109038), Istradefylline (Lot No.: E1624040), Panobinostat (Lot No.: D1510023), Rolapitant (Lot No.: F2214052), Tasimelteon (Lot No.: H2118249), Vorapaxar (Lot No.: G2216638), Fedratinib (Lot No.: E1719007), Lenvatinib (Lot No.: J1520104), Pomalidomide (Lot No.: F1524104), Ruxolitinib (Lot No.: C1926101), Telaprevir (Lot No.: F1515073), Baricitinib (Lot No.: B1512012), Macitentan (Lot No.: H1507106), Safinamide (Lot No.: E1529132), Tofacitinib (Lot No.: I1925019), Bosutinib (Lot No.: B1512016), Sonidegib (Lot No.: S215103), and Testosterone (Lot No.: F2126139). Additionally, Flibanserin (Lot No.: 17354), and Edoxaban (Lot No.: 41922) were obtained from MedChemExpress, and Tolbutamide (Lot No.: BCCF4700) was purchased from Sigma-Aldrich. Ketoco-

nazole (Lot No.: LF90U63) was purchased from J&K Scientific. Ultrapure water was produced using an Ultrapure-Water Generating System, and PBS (PH7.4) was purchased from BasalMedia. Finally, HLM (Lot No.:2010065) were purchased from XenoTech.

In vitro **experiments for determination off_m**

To prepare for the experiment, 33 compounds, positive controls, and inhibitors were dissolved in DMSO to create 10 mM stock solutions, which were then stored at -40 . Prior to the experiment, NADPH was dissolved in PBS to create a 3 mM working solution. HLM stock solution was diluted with PBS, and a certain volume of organic solvent, compound, positive control, or inhibitor was added to create HLM working solution, HLM inhibitor (15 μM) working solution, HLM compound (3 μM) working solution, and HLM positive control (3 μM) working solution. All these working solutions contained 0.75 mg mL^{-1} HLM.

To create the non-reaction control group, HLM working solution was mixed with a 3 μM compound or positive control working solution in equal volume. The non-inhibition group was created by mixing HLM working solution with a 3 μM compound or positive control working solution in equal volume. The inhibition group was created by mixing the HLM inhibitor working solution with a 3 μM compound or positive control working solution in equal volume. These reaction groups were preheated at 37 for 5 minutes, and then the same volume of NADPH working solution was added for the reaction. Prior to starting the reaction, 3 times the volume of ACN termination solution containing 20 ng mL^{-1} internal standard was added to the non-reaction control group to terminate the reaction, and it was then stored at -40 . The other two groups were incubated at 37 at 150 rpm for 60 minutes. At the end of the reaction, 3 times the volume of ACN termination solution containing 20 ng mL^{-1} internal standard was added to terminate the reaction.

After the reaction, the reaction plate was shaken at 600 rpm for 10 minutes and then centrifuged at 6000 rpm for 15 minutes. The supernatant was collected for LC-MS/MS analysis.

HPLC-MS analysis for determination of plasma concentrations

The supernatant were analyzed using a liquid phase system, which included the Waters ACQUITY Ultra Performance Liquid Chromatography I-Class Plus system, equipped for the analysis of Bosutinib, Nintedanib, Rivaroxaban, Apixaban, and Vilazodone, as well as a High Performance Liquid Chromatography system (Shimadzu LC), used for the analysis of Fostamatinib, Ponatinib, Axitinib, Crizotinib, Venetoclax, Ibrutinib, Sonidegib, Roflumilast, Suvorexant, Apremilast, Elagolix, Istradefylline, Panobinostat, Rolapitant, Tasimelteon, Fedratinib, Lenvatinib, Pomalidomide, Ruxolitinib, Ospemifene, Edoxaban, Baricitinib, Vorapaxar, Flibanserin, Macitentan, Safinamide, and Tofacitinib. Separation of the analytes was achieved using a reversed-phase ACE T3 column (1.8 μm, 2.1×50 mm) and the mobile phase consisted of 0.1% formic acid in water for the A phase and 0.1% formic acid in acetonitrile for the B phase. The samples concentrations were then determined using a Triple Quad 6500+ mass spectrometer (Applied Biosystems, USA), equipped with electron spray ionization (ESI) and a tandem quadruple mass analyzer. Data processing was performed using Analyst software (SCIEX), and the mass spectrum parameters can be found in Table S1.

Part II

The calculation of Cl_{int} values andf_m

The f_m can be calculated by comparing the*in vitro* clearance in the presence of an inhibitor to that in its absence. To determine the Cl_{int} of a drug in the absence of ketoconazole, its concentration at each time point can be measured using the HMPL-MS method. The initial rate of drug disappearance can then be calculated by using linear regression of the concentration versus time data, which yields the slope value, k. This value can be used to determine the *in vitro* Cl_{int} by the following formula:

$$Cl_{int}\ (\text{mL min}^{-1}\text{mg}^{-1}) = \frac{k(\text{min}^{-1})}{\text{Concentration of liver microsomes(mg mL}-1\ )}$$

To measure the Cl_{int} in the presence of ketoconazole, the inhibitor is added to the microsomal incubation, and the same procedure is repeated. The presence of the inhibitor reduces the metabolism reaction, resulting in a lower Cl_{int} value. The f_m can be calculated using the formula:

$f_m = \frac{CLintwithout\ inhibitor CLintwith\ inhibitor}{\text{CLintwithout inhibitor}}$

Prediction of in silico f_m

The f_m can be also calculated based on predicted major CYP enzyme kinetics (*in vivo* K_m and V_{max}), combining compound's structure and quantitative structure activity relationship (QSAR) model defaulted in ADMET Predictor module of GastroPlus. The clearance of each enzyme ($Cl_{CYP,i}$) is expressed as the Mieman equation:

$Cl_{CYP,i} = V_{max,i} / (K_{m,i} + S)$

Then the f_m of CYP3A4 (that is in silicof_m) could be shown in GastroPlus using the Cl_{CYP3A4} divided by the sum of $Cl_{CYP,i}$for each enzyme contributed on drug metabolism.

The PBPK model of ketoconazole

The PBPK model of ketoconazole has been developed and validated in my published paper (Ren, Sai, Chen, Zhang, Tang & Yang, 2021). The model parameters and validation results are summarized in Table S2 and Figure S1, respectively. This PBPK model was used to predict DDIs in line with the study's findings.

The PBPK model of substrates

In our previous work, we reported the primary modeling parameters and fundamental PK models for 33 compounds. In this study, we utilized the*in vitro* measured f_m value to characterize the contribution of the CYP3A4 enzyme to liver clearance. As a result, we updated the clearance in the PBPK model from

$Cl_{sys} = Cl_{CYP3A4} + Cl_R$

to

$Cl_{sys} = Cl_{CYP3A4} + Cl_{other} + Cl_R$

where Cl_{sys} is the total *in vivo* clearance, Cl_{CYP3A4} is the clearance mediated by CYP3A4, Cl_{other} is the clearance mediated by other metabolism enzymes, and Cl_R is the clearance mediated by the kidney. The PBPK models of the substrates after administration alone were validated by visual comparison of the coincidence between the predicted PK curve and the clinical observations as showed in Figure S2.

To define *in vitro* f_m in the PBPK models, we assumed that it conforms to linear dynamics in the Mieman equation, which means assigning a value much larger than S to K_m. As a result, the initial V_{max} can be calculated simply using the following formula, and the final V_{max} was fitted by comparing the f_m of CYP3A4 in the updated PBPK models with corresponding *in vitro* f_m as well as evaluating the performance of PK predictions.

$V_{max} = Cl_{CYP3A4} \cdot K_m$

Prediction of DDI

The PBPK modeling of above drugs and the DDI module of GastroPlus were utilized to predict the potential pharmacokinetic (PK) changes that may occur when combining a substrate and ketoconazole. After confirming the PBPK models of the substrate and inhibitor, we used the DDI module of GastroPlus to predict the potential PK changes resulting from the combination of the two compounds. The DDI module accounted for the clearance of the substrate, which includes three components: the metabolism of CYP3A4 (with its f_m value determined via *in vitro* experiments), the metabolism of non-CYP3A4 enzymes, and renal excretion. We used the default inhibition constant of CYP3A4 (Ki = 0.015 μM) in the PBPK model of ketoconazole. The administration regimen for the combination of the substrate and inhibitor were summarized in Table S3. Using the dynamics of substrates and Ketoconazole, we simulated the DDI potential based on the dynamics, Ki value, and f_m . The DDI potential was calculated using the following equations:

$T_{max}R = T_{max,\ i}/T_{max}$

$C_{max}R = C_{max,\,i}/T_{max}$

$AUCR = AUC_i$ / AUC

where $T_{max,\,i}$, $Cmax_{,\,i}$, and AUC_i are the parameters of drugs when co-administered with ketoconazole, and T_{max}, C_{max}, and AUC are the parameters of the drug when administered alone.

Evaluation of the predictive performance

The predictive performance was evaluated by comparing the predicted AUCR, $C_{max}R$, and $T_{max}R$ with the observed ratios. Deviation of up to 0.5-2 folds of the observed geometric mean ratio (GMR) was considered acceptable for predictions. Predictions falling within the 90% confidence interval of the observed GMR indicated an exact prediction.

RESULTS

Case details of enrolled victim drugs

A total of 33 drugs, approved by the FDA between 2011 and 2020, were enrolled for evaluation of predictive performance after meeting specific screening criteria. To be eligible, these drugs were required to have available pharmacokinetic profiles when administered alone or co-administered with ketoconazole, as well as available ADME properties. The structure of these 33 compounds is presented in Figure S3, and their characteristics and statistics are listed in Table 1. The DDI potentials of the drugs were divided into two categories based on the 90% confidence interval of AUCR, where 15 out of the 33 compounds had AUCR<2, accounting for 45% of the total. Table 1 shows that there were no significant differences between the two categories in terms of logP, P_{eff}, BP, V_{ss},f_u , and Cl_R. However, compounds with AUCR>2 tended to have higher Cl_{liver}(Cl_{CYP3A4} + Cl_{other}) and *in vivo*f_m . A correlation analysis of Cl_{liver}, *in vitro* f_m , and AUCR was performed using a 3-D plot as showed in the Figure 1, which indicated that compounds with higher Cl_{liver} and*in vitro* f_m had higher AUCRs. Out of 33 compounds co-administered with ketoconazole, six victim drugs experienced an increase in exposure of more than three times. All six of these victim drugs have a high Cl_{liver} (>15 L h^{-1}) and a high f_m(>75%). Conversely, the 18 drugs with lower clearance rates (<15 L h^{-1}) among the 33 compounds showed an increase in exposure of less than three times after being co-administered with ketoconazole, regardless off_m .

Estimation of f_m of victim drugs by human microsomes

In this study, we measured changes in intrinsic clearance of 33 compounds in HLM, with and without ketoconazole, using the substrate depletion method to evaluate the fraction metabolized by CYP3A4 for these drugs. Figure S4 illustrates a moderate positive correlation between *in vitro* Cl_{int} and Cl_{liver} without inhibitors, indicating the reliability of this method. In addition to the above *in vitro* method, we also used *in vivo* and in silico prediction methods to determinef_m . We calculated *in vivo*f_m using a PBPK-DDI model, by matching the simulated DDI PK data of the test article to the observed DDI PK data. We predicted in silico f_m using computational methods based on the drug's molecular structure, using ADMET Predictor module. The findings of our study are presented in Table 2, which includes reported *in vitro* findings, phenotyping study conclusions, and tested *in vivo* , *in vitro* , and in silicof_m values, compared across three different approaches. The *in vitro* f_m results were consistent with the reported *in vitro* $f_m$or phenotyping study conclusions. However, weak correlations were observed between the *in vivo* f_m and in silico f_m values, as well as the *in vitro*results (showed in the Figure S5). As previously mentioned, drugs with higher Cl_{liver} are more likely to cause DDIs and are more sensitive to changes in metabolic parameters such asf_m . To investigate this further, we compared the*in vitro* f_m minus *in vivo*f_m values between drugs with Cl_{liver} above and below 15 L h^{-1}, as well as the predicted in silico f_m minus *in vivo* f_m values. Figure 2 indicate that drugs with a Cl_{liver} higher than 15 L h^{-1}exhibit smaller variations of predicted in silicof_m minus *in viv* o $f_m$and *in vitro* f_m minus *in vivo*f_m compared to drugs with a Cl_{liver} lower than 15 L h^{-1}. Furthermore, when comparing drugs with a Cl_{liver} higher than 15 L h^{-1}, the difference between the *in vitro* f_m and *in vivo* f_m was smaller than that between in silico and *in vivo*f_m . These results suggest that *in vitro* f_m measurements may provide more accurate predictions of DDI, particularly for drugs with higher Cl_{liver}.

Predictive performance of the PBPK-DDI model

The PBPK-DDI model was used to predict DDI results by incorporating different f_m s, such as in silico, 100%, and*in vitro* f_m . The results were presented in Figures 4, 5, and 6, showing predicted AUCR, $C_{max}R$, and $T_{max}R$ values. Notably, the predicted $T_{max}R$ was found to be accurate within 2 times the observed $T_{max}R$ when using in silico or *in vitro* f_m methods, but not with 100%f_m . The PBPK model utilizing *in vitro* f_m data outperforms the other two values off_m in predicting $C_{max}R$ and AUCR, as demonstrated by the close proximity of the predicted values to the unit line (y=x) compared to the 100% f_m and in silico f_m integrated PBPK-DDI model. As a summary, *in vitro* f_m was the most precise method, as it accurately predicted the $C_{max}R$ of 31 drugs within 2 times of the measured results, and the AUCR of 28 drugs within 2 times of the measured results. In contrast, the use of 100%f_m and in silico f_m led to lower prediction accuracy. Only 24 drugs had their $C_{max}R$ predicted within 2 times of the measured results when using 100%f_m or in silico f_m , and 26 drugs for $C_{max}R$ when using in silicof_m . Similarly, only 24 and 25 drugs for AUCR were predicted within 2 times of the measured $C_{max}R$ when using 100% f_m or in silicof_m , respectively. The findings demonstrate that incorporating *in vitro* f_m data into PBPK models significantly enhances the accuracy of predicting the extent of DDIs for the parameters studied. While in silico f_m shows some promise, its impact on prediction is limited.

DISCUSSION

Accurate prediction of potential DDIs is crucial in ensuring patient safety and efficacy of drugs during the drug discovery and development process. PBPK-DDI models rely on the accurate representation of various physiological parameters and processes to predict the DDIs. We used two methods to determine the metabolism and f_m of test articles for improvement of DDI prediction are as follows: i) *In vitro*approach using HLM. This method directly measures the fraction metabolized by simulating the metabolic process in the human liver. ii) in silico approach using mathematical models. This method predicts the metabolism and f_m based on the molecular structure and properties of the substance, without the need for laboratory experimentation. By incorporating differentf_m values by *in vitro* method or in silico method, instead of assuming 100% values, the accuracy of PBPK models can be improved, leading to more precise predictions. The use of actual*in vitro* determined values for predicting DDIs leads to improved accuracy compared to using in silico methods. This can help to better understand the pharmacokinetics of drugs in different populations and inform drug development and regulatory decisions.

In addition to liver microsomes, other *in vitro* systems such as hepatocytes and recombinant enzymes can be used to determine the metabolic fate of drugs, f_m , and evaluate their potential for DDIs (Lindmark, Lundahl, Kanebratt, Andersson & Isin, 2018; Youdim et al., 2008). Each system has its own advantages and limitations, and the choice of system depends on the specific research question being addressed and the properties of the drug under investigation. Hepatocytes contain a much broader range of metabolic enzymes such as alcohol dehydrogenase (ADH) and aldehyde dehydrogenase (ALDH), which are involved in the metabolism of alcohol, and glucuronosyltransferases, sulfotransferases, and glutathione S-transferases (Klammers et al., 2022; Lindmark, Lundahl, Kanebratt, Andersson & Isin, 2018). Herein, the hepatocytes have been considered better for *in vitro* evaluation on f_m as they provide a more accurate representation of the metabolic activities of the liver (Lindmark, Lundahl, Kanebratt, Andersson & Isin, 2018). However, microsomes are still widely used due to their ease of preparation, cost-effectiveness, and stability, and they still provide valuable information about drug metabolism and evaluation onf_m . In this paper, the prediction of DDIs using the PBPK-DDI model with incorporation of $f_m$values from HLM is relatively accurate and does not significantly overestimate the results. Since most of these drugs are primarily metabolized by the P450 enzyme system in the liver, the *in vitro*studies using HLM can provide a good prediction of the potential for DDIs *in vivo* . If other enzymes, such as ADH, ALDH, glucuronosyltransferases, sulfotransferases, and glutathione S-transferases are involved into drug metabolism, hepatocytes are a better choice for determining the f_m as they contain these various enzyme systems and can provide a comprehensive view of the drug metabolism process.

The study found that Cl_{liver} and fraction metabolized by CYP3A4 are significant factors in understanding

DDI as showed in Table 1 and Figure 1. Drugs with high Cl_{liver} are more likely to be affected by CYP3A inhibitors, which can result in changes in the drug's exposure and potential interactions. There is total 6 victim drugs which exposure increased higher than 3 times among 33 compounds when co-administered with ketoconazole and all of these six victim drugs possess higher Cl_{liver} (>15 L h^{-1}). On the other hand, drugs with low Cl_{liver} may not see significant changes in clearance when exposed to CYP3A inhibitors as the body's elimination processes for the drug are already at their limit. There are 18 drugs with lower Cl_{liver} (<15 L h^{-1}) among the 33 drugs and their exposure increase less than 3 times after co-administered ketoconazole. When the f_m is low, it indicates that the CYP3A isoform is not a major contributor to the metabolism of a drug, and therefore, inhibitors of CYP3A such as ketoconazole may not have a significant effect on the metabolism of the drug. Herein, the above 6 victim drugs with exposure increased higher than 3 times not only possess higher clearance (>15 L h^{-1}) but also higher f_m(>75%).

The tested f_m values from the two methods are not consistent with the actual, real-life conditions of the biological system being studied, as showed in Figure S5. It seems to indicate a problem with the methods used or a limitation in the ability of the methods to accurately reflect the true situation *in vivo* . However, the predictions of DDIs were improved much by integration of*in vitro* f_m , which are indeed more accurate than predictions based on in silico f_m or 100% off_m . The underlying cause of this phenomenon is that variation between *in vitro* and *in vivo* measurements of f_m is lower than that between in silicof_m and *in vivo* f_m for the drugs with high clearance as showed in Figure 2. The difference between*in vitro* f_m and *in vivo* $f_m$is unlikely to have a significant impact on the assessment of potential DDIs since the evaluation of low-clearance compounds for DDIs is not sensitive to variations in f_m . The discrepancy between *in vitro* and *in vivo* measurements off_m is always observed for compounds with low clearance. The lower the clearance value, the slower the rate of drug metabolism, leading to smaller changes in drug concentration in HLM system. The limited accuracy of detection (±15%) can make it challenging to determine the effect of inhibitors on the drug's metabolism.

We used the remaining amount of substrate and *in vitro* clearance as an index to calculate the fraction metabolized by CYP3A4 with or without an inhibitor respectively. The first method is simple and straightforward and provides a rough estimate of the fraction metabolized by CYP3A4 by using the remaining amount of substrate as an index. On the other hand, the second method provides a more controlled and direct way to evaluate the metabolic fate of the substrate by measuring the rate of metabolism in a laboratory setting and provide more accurate and precise results compared to the first method.

It is important to note that abiraterone and naloxegol were not enrolled in this paper. Abiraterone is a pro-drug, which metabolism process may involve multiple enzyme systems. Therefore, a more comprehensive evaluation of multiple enzyme systems is necessary to accurately assess the f_m of abiraterone. The present PBPK-DDI model considers the metabolic pathways and enzymes involved in drug metabolism, but transporters also play a significant role in DDIs and cannot be overlooked. Naloxegol is a substrate for both CYP3A and a transporter, the developed PBPK-DDI model may not accurately predict the potential for DDI, as the interplay of metabolic and transport mechanisms is complex. The DDI risk of naloxegol is obviously under-estimated using the PBPK-DDI model. Therefore, it may further improve the prediction to consider both metabolic and transport mechanisms when evaluating the potential for DDIs, to provide a more comprehensive understanding of the interactions between drugs.

CONCLUSION

In conclusion, our study highlights the importance of incorporating*in vitro* f_m data into PBPK models to improve the accuracy of predicting DDIs. While in silico $f_m$may have some potential, its influence on predictions appears to be limited. Our findings suggest that drugs with high Cl_{liver} levels (>15 L·h^{-1}) and high f_m(>75%) are particularly susceptible to the impact of CYP3A4 inhibitor ketoconazole, highlighting the need for further research to better understand the relationship between clearance,f_m , and the risk of CYP3A4 drug-drug interactions. By improving our ability to predict DDIs, our research has the potential to enhance drug safety and efficacy, ultimately benefiting patient health.

ACKNOWLEDGMENTS

The authors thank Simulations Plus, Inc. (Lancaster, CA, USA) for authorizing the use of the optimization module in this study. We thank Zhuo-jing Wu (Jinzhou Medical University, Jinzhou, China) for preparation of the graphical abstract.

AUTHOR CONTRIBUTIONS

Hong-can Ren, Lily Tang, Hong Wan, and Ming Li designed the research; Jiang Pin, Lin-Feng Chu, and Ren-Peng Xu completed the determination off_m ; Tao Chen, Hong-can Ren, Jin-ting Gao, Li Wang, and Qiang Liu analyzed the data; Hong-can Ren, Pin Jiang, and Tao Chen wrote the manuscript; and Lily Tang, Hong wan, and Ming li revised the manuscript.

REFERENCES

Gertz MA, & Dispenzieri A (2020). Systemic Amyloidosis Recognition, Prognosis, and Therapy: A Systematic Review. JAMA 324: 79-89.

Gomez-Mantilla JD, Huang F, & Peters SA (2023). Can Mechanistic Static Models for Drug-Drug Interactions Support Regulatory Filing for Study Waivers and Label Recommendations? Clin Pharmacokinet 62: 457-480.

Klammers F, Goetschi A, Ekiciler A, Walter I, Parrott N, Fowler S, et al. (2022). Estimation of Fraction Metabolized by Cytochrome P450 Enzymes Using Long-Term Cocultured Human Hepatocytes. Drug Metab Dispos 50: 566-575.

Lin W, Chen Y, Unadkat JD, Zhang X, Wu D, & Heimbach T (2022). Applications, Challenges, and Outlook for PBPK Modeling and Simulation: A Regulatory, Industrial and Academic Perspective. Pharm Res 39: 1701-1731.

Lindmark B, Lundahl A, Kanebratt KP, Andersson TB, & Isin EM (2018). Human hepatocytes and cytochrome P450-selective inhibitors predict variability in human drug exposure more accurately than human recombinant P450s. Br J Pharmacol 175: 2116-2129.

Lu X, Horner JW, Paul E, Shang X, Troncoso P, Deng P, et al. (2017). Effective combinatorial immunotherapy for castration-resistant prostate cancer. Nature 543: 728-732.

Murayama N, Yajima K, Hikawa M, Shimura K, Ishii Y, Takada M, et al. (2018). Assessment of multiple cytochrome P450 activities in metabolically inactivated human liver microsomes and roles of P450 2C isoforms in reaction phenotyping studies. Biopharm Drug Dispos 39: 116-121.

Ren HC, Sai Y, Chen T, Zhang C, Tang L, & Yang CG (2021). Predicting the Drug-Drug Interaction Mediated by CYP3A4 Inhibition: Method Development and Performance Evaluation. AAPS J 24: 12.

Shebley M, Sandhu P, Emami Riedmaier A, Jamei M, Narayanan R, Patel A, et al. (2018). Physiologically Based Pharmacokinetic Model Qualification and Reporting Procedures for Regulatory Submissions: A Consortium Perspective. Clin Pharmacol Ther 104: 88-110.

Watanabe R, Kawata T, Ueda S, Shinbo T, Higashimori M, Natsume-Kitatani Y, et al. (2023). Prediction of the Contribution Ratio of a Target Metabolic Enzyme to Clearance from Chemical Structure Information. Mol Pharm 20: 419-426.

Yang X, Pfuma Fletcher E, Huang SM, Zineh I, & Madabushi R (2021). Regulatory Efforts to Facilitate Evaluation and Clinical Management of Drug-Drug Interaction Risks. Clin Pharmacol Ther 109: 42-46.

Youdim KA, Zayed A, Dickins M, Phipps A, Griffiths M, Darekar A, et al. (2008). Application of CYP3A4 in vitro data to predict clinical drug-drug interactions; predictions of compounds as objects of interaction. Br J Clin Pharmacol 65: 680-692.

FIGURE LEGENDS

Figure 1. 3-D Scatter Plot of the Cl_{liver}, *in vitro* f_m , and the AUCR. Red balls in the 3-D scatter plot represent 33 compounds positioned according to their corresponding values of Cl_{liver}, *in vitro* f_m , and AUCR. Green points in the plot show the projection of the red balls onto the AUCR-Cl_{liver} plane, demonstrating the relationship between Cl_{liver} and AUCR, independent off_m . Similarly, blue points in the plot indicate the projection of the red balls onto the AUCR-$f_m$plane, indicating the relationship between f_m and AUCR for each compound, independent of Cl_{liver}.

Figure 2. Comparison of *in vitro* and in silico predictions off_m accuracy with *in vivo* values for compounds with a Cl_{liver} higher than 15 L h^{-1}. The boxplot on the left depicts the difference between f_m *in vitro* andf_m *in vivo* , while the boxplot on the right displays the difference between f_m in silico andf_m *in vivo* .

Figure 3. Comparison of T_{max}R predictions made using three different f_m s with the measured T_{max}R values. The left panel assumes a fixedf_m value of 100%, the middle panel uses an in silico f_m , and the right panel uses an *in vitro* f_m

Figure 4. Comparison of C_{max}R predictions made using three different f_m s with the measured C_{max}R values. The left panel assumes a fixedf_m value of 100%, the middle panel uses an in silico f_m , and the right panel uses an *in vitro* f_m

Figure 5. Comparison of AUCR predictions made using three differentf_m s with the measured AUCR values. The left panel assumes a fixed f_m value of 100%, the middle panel uses an in silico f_m , and the right panel uses an *in vitro* f_m

TABLE CAPTIONS

Table 1. Characteristics and Statistics of Victim Drugs, Categorized by AUCR. AUCR<2 denotes cases where the upper limit of the 90% confidence interval (95% quantile) is within 2 times, while AUC>=2 represents cases where the upper limit of the 90% confidence interval (95% quantile) is greater than or equal to 2 times.

Table 2. Comparison of f_m Values Obtained by Three Different Methods and Literature Reports. *In vitro* f_m represents the f_m value obtained by the *in vitro* microsome method, in silicof_m represents the f_m value based on computer prediction, and *in vivo* $f_m$represents the f_m values obtained from actual DDI results using the PBPK model.

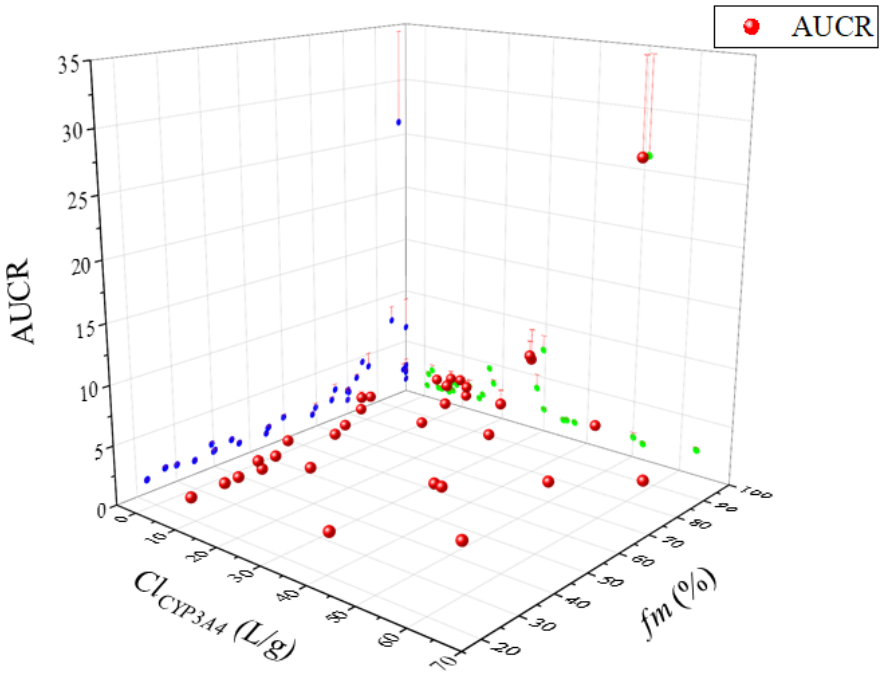

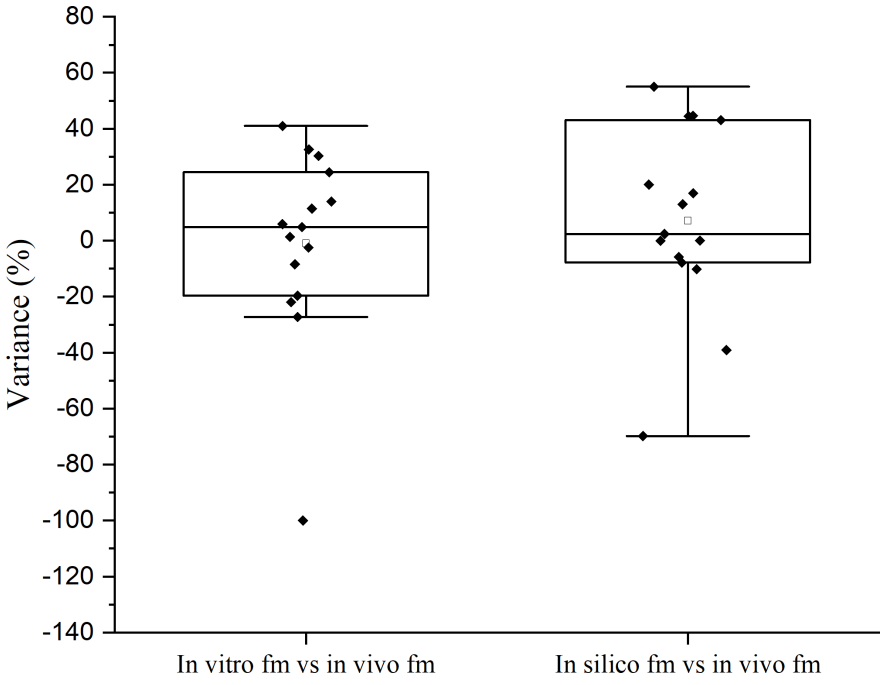

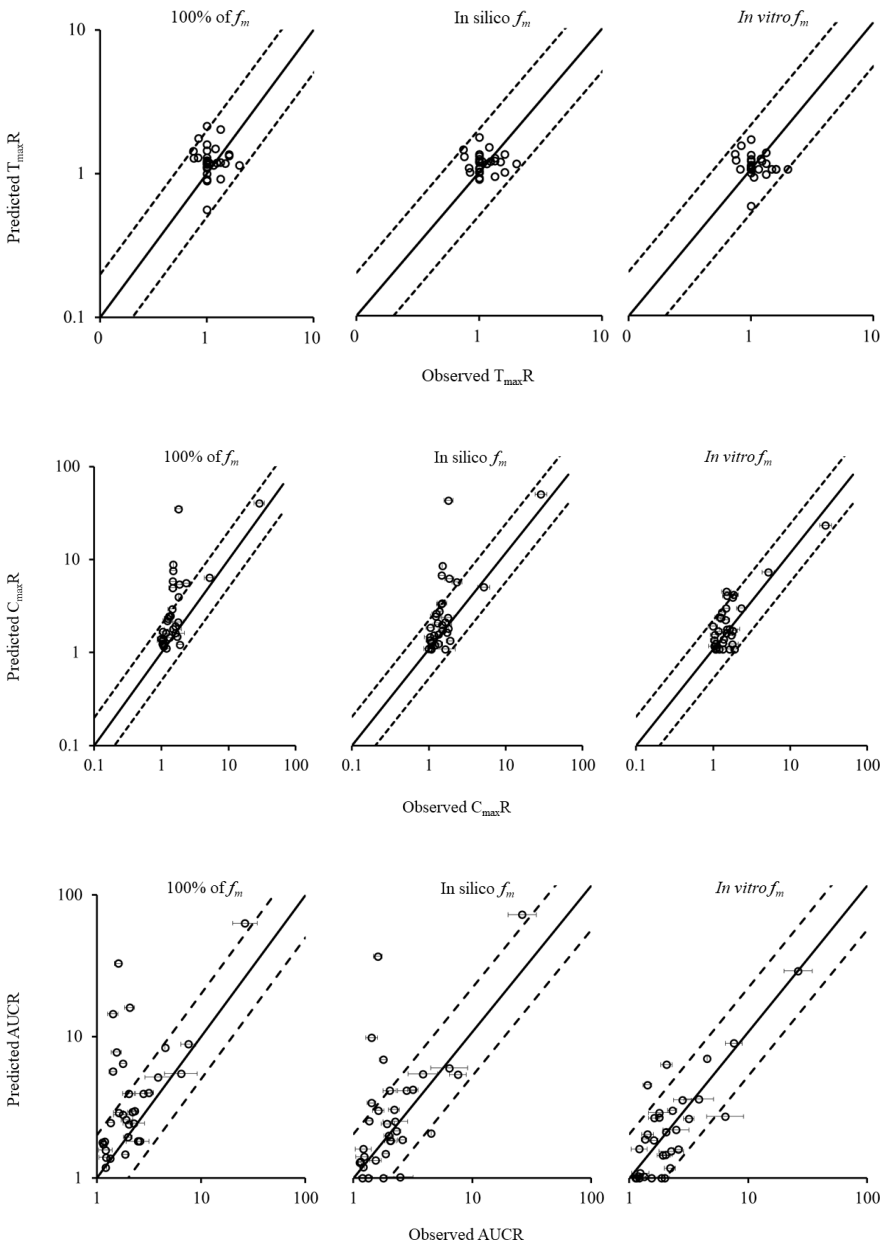

Hosted file

`Table 1.xlsx` available at https://authorea.com/users/607355/articles/636079-enhancing-drug-drug-interaction-prediction-by-integrating-physiologically-based-pharmacokinetic-model-with-fraction-metabolized-by-cyp3a4

Hosted file

`Table 2.xlsx` available at https://authorea.com/users/607355/articles/636079-enhancing-drug-drug-interaction-prediction-by-integrating-physiologically-based-pharmacokinetic-model-with-fraction-metabolized-by-cyp3a4